PCCP

PERSPECTIVE

View Article Online
View Journal | View Issue

Cite this: *Phys. Chem. Chem. Phys.*, 2020, **22**, 13850

Towards sustainable and efficient p-type metal oxide semiconductor materials in dye-sensitised photocathodes for solar energy conversion

Sina Wrede and Haining Tian *

Received 10th March 2020,
Accepted 27th May 2020

DOI: 10.1039/d0cp01363c

rsc.li/pccp

In order to meet the ever-growing global energy demand for affordable and clean energy, it is essential to provide this energy by renewable resources and consider the eco-efficiency of the production and abundance of the utilised materials. While this is seldom discussed in the case of technologies still in the research stage, addressing the issue of sustainability is key to push research in the right direction. Here we provide an overview of the current p-type metal oxide semiconductor materials in dye-sensitised photocathodes, considering element abundance, synthetic methods and large scale fabrication as well as the underlying physical properties that are necessary for efficient solar harvesting devices.

1 Introduction

Today, concerns surrounding the causes and consequences of man-made climate changes are central topics in our everyday lives. The global attention to this issue has increased drastically and the demand for a sustainable future is now larger than ever. In order to make such a future our reality, society has to make the transition from fossil-fuel resources to sustainable renewable energy alternatives and cope with the steadily increasing energy demand at the same time. It is predicted that the global energy demand is going to double by 2050 with the main contribution coming from the rise of developing countries.[1,2] In particular, Asia is at the forefront due to the economic growth, infrastructure development, population growth and access to electricity for a new segment of the population. In order to achieve a socially just and equitable future, it is imperative that this increase is to be met with a sustainable solution allowing developing countries to increase their living standards.

Department of Chemistry-Ångström Lab., Uppsala University, Box 523, 75120 Uppsala, Sweden. E-mail: haining.tian@kemi.uu.se

Sina Wrede

Sina Wrede obtained her bachelor's degree in chemistry from Ludwig-Maximilians Universität (LMU), München (Germany), in 2017 and her MSc degree in chemistry from Uppsala University (Sweden) in 2019. Currently she is working as a PhD student in Prof. Haining Tian's group at Uppsala University. Her research focuses on p-type dye-sensitised photocathodes for solar energy conversion and storage.

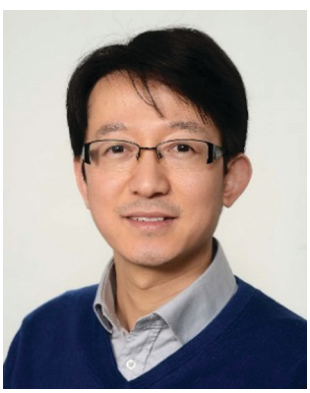

Haining Tian

Haining Tian is an Associate Professor with sepcialization in photoactive nanomaterials at Uppsala University, Sweden, leading a research group of Molecular Devices for Artificial Photosynthesis. He obtained his PhD in Applied Chemistry at Dalian University of Technology (DUT) in 2009 and then moved to Royal Institute of Technology (KTH) as a Postdoc/senior researcher until 2014. He has been awarded the Göran Gustafsson Prize for young researchers (2016 and 2020), Young Investigator from European Photochemistry Association (2019) and Wallenberg Academy Fellow (2019). His research interests focus on development and investigation of sustainable materials for solar energy conversion and storage.

Fig. 1 In order to achieve the Sustainable Development Goal (SDG) number 7, affordable and clean energy, that world leaders have agreed upon in 2015, this energy needs to come from sustainable devices produced by renewable resources and other selection parameters.

Out of the several renewable energy sources, such as wind, tidal or biomass energy, solar energy is one of the most promising resources due to its abundance and omnipresence. It is estimated that the world's total energy use equals only approximately 0.00015% of the solar energy reaching the earth.[3] Furthermore, solar energy can be converted into both electricity and fuels, which makes its storage and transport over long distances easier. In order to fully transit into a carbon free future, the development of solar harvesting is inevitable and needs to reach large-scale deployment, taking the scalability, safety, efficiency and durability into consideration, as illustrated in Fig. 1. Most of the research today focuses mostly on improving the efficiency of devices without taking other selection parameters into consideration. However, the energy demand during production, durability and cost of maintenance of the system can mitigate or compensate extra costs and are therefore important factors to keep in mind during the development of new solar cell and solar fuel devices.

In this perspective, the concept of sustainability is discussed within the field of solar harvesting for solar cells and solar fuel devices with a focus on photocathodes by discussing the current semiconductor materials and their energy costs to identify sustainable electrode candidates considering element abundance, costs and toxicity.

2 Dye sensitised photocathodes for solar cells and solar fuels

Like any other emerging technology in our economy centred society, the success of solar harvesting devices depends mostly on the production costs which are determined by the fabrication process and material costs. While the material costs are mostly driven by the material abundance, it is also important to consider the sustainability and renewability of materials that are used in devices with such a large market and volume in the upcoming years.

2.1 Element abundance and life cycle assessment

With a predicted power demand of around 30 TW by 2050,[4] solar harvesting devices will have to expand drastically to meet this energy demand. However, terawatt-scale realisation requires a massive amount of natural resources which can prevent reaching this scale due to limited resource supply.[5] For current solar cell technologies, Tao *et al.*[5] examined the resource limitations that would arise for the terawatt-scale in order to meet a fraction of our power demand from solar energy harvesting. For example, the terawatt-scale for CIGS or CIS ($CuIn_xGa_{1-x}Se_2$) solar cells will be hindered by the limited indium reserves, as well as a production bottleneck for gallium, which only exists in very small concentrations in other ores.[5] CdTe solar cells will be limited by the availability of tellurium, and the current silicon solar cell technology at such a scale would deplete the silver reserves in only two decades according to Tao (for silver electrodes). This underlines the importance of making the existing technologies more sustainable and exploring new alternatives. For dye-sensitised solar cells, consisting mostly of TiO_2 or NiO, which are vastly earth abundant, resource limitations are less critical, especially if an organic dye instead of a ruthenium containing dye is utilised. Most affected by natural resource limitations are materials that use metals that are at supply risk, which often are available largely as byproducts and possess no effective substitutes, as shown in Fig. 2.[6] It should be kept in mind that forecasting the availability of materials is not easy and fluctuations can occur, nonetheless, metal availability is a key factor to consider for solar harvesting technologies that are aimed at large-scale production. However, due to the need for the large-scale production of a variety of solar harvesting devices, there is no doubt that some elements that are considered "critical" will be unavoidable and recycling will become more important than ever.

Another limitation for crystalline-Si solar cells, which have the highest solar conversion efficiencies, is the large amount of energy required to fabricate these cells due to the energy intensive process of making Si-wafers. However, amorphous-Si (a-Si) solar cells only need a fraction of the production energy of crystalline-Si solar cells.[5] Despite this, they require more production energy than other thin-film technologies. However,

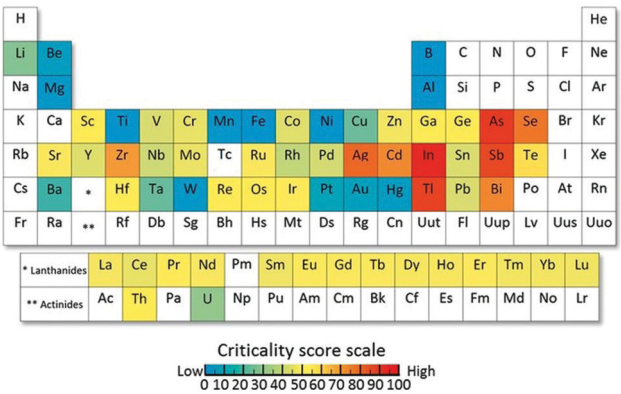

Fig. 2 Periodic table of endangered elements showing the global level for supply risk of 62 metals that were investigated. Elements that are shown in blue are vastly abundant or biomass elements, which are naturally recycled (such as Ti, Mn, Fe and Al) and elements in red are elements that are at supply risk in the near future. Reproduced with permission from National Academy of Sciences.[6]

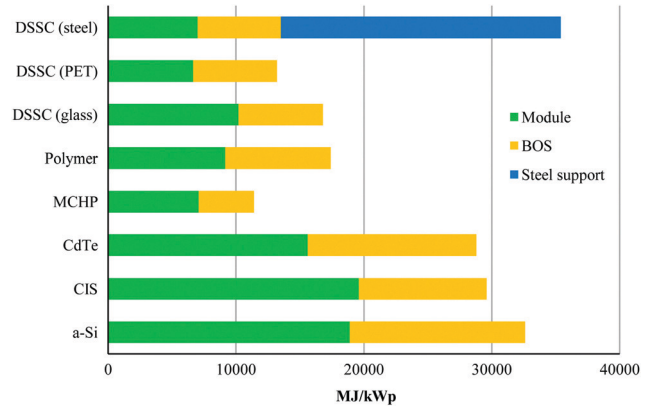

Fig. 3 Cumulative energy demand for the production of a virtual 3 kW h solar harvesting rooftop photovoltaic installation for various thin-film technologies. Reproduced with permission from Elsevier.[7]

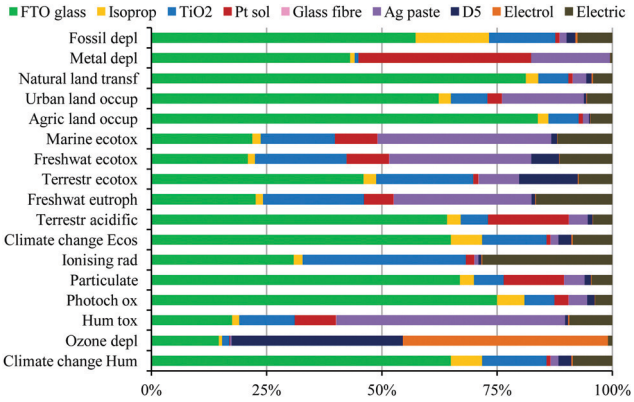

Fig. 4 Characterisation diagram of the environmental profile for the different device components in the manufacturing process of a virtual module with the organic D5 dye and I^-/I_3^- liquid electrolyte. Reproduced with permission from Elsevier.[7]

a multijunction of the two materials (amorphous silicon + crystalline silicon), so-called micromorph solar cells (MCHP), gives the lowest production energy demand.[7] Fig. 3 shows the Cumulative Energy Demand (CED) for a virtual 3 kWp roof-top integrated installation of various thin-film technologies that is the result of a life-cycle assessment of up-scaled solar applications, which shows that DSSCs are clearly competitive with other thin-film technologies.[7] While it is clear that the CED varies significantly for different types of materials, as well as their contribution to the BOS, Balance of System (*i.e.*, module supports, cabling, and power conditioning), it should be noted that the additional energy demand for the steel support is based on a prototype which has the double function of roofing and supporting the dye-sensitised solar cells (DSCs or DSSCs). However, this large contribution demonstrates the importance of integrating solar harvesting systems into already available housing supports or a support with double function to avoid unnecessary additional energy for a module support.

Despite this life-cycle analysis for a roof-top installation to compare these thin-film technologies, it must be kept in mind that the potential application for these thin-film technologies can be quite different and not all are best suited for roofing since their strengths lie elsewhere. Dye-sensitised devices, for example, are one of the few technologies that are transparent and colourful which make them a unique and feasible candidate for integrated photovoltaic architectural elements, such as windows.[8] Even in a standard glass dye-sensitised device, FTO glass is the main factor that contributes to the energy production cost and life cycle impact of the DSSCs. Despite the fact that glass can be easily and efficiently recycled, it would be great if the additional costs for support are handled by the support of the window. Ideally, the environmental impact of such devices could be even lower since a large impact of the module comes from the FTO glass substrate (see Fig. 4), which could have double function for the glass of the window, making the whole system 'greener'. The same is true for dye-sensitised photoelectrochemical cells (DS-PEC) for solar fuel production, which only need one substrate onto which the semiconductor is applied, making them an attractive candidate for solar fuel production. While no life-cycle analysis has been performed for DS-PEC, a more general life cycle assessment for large-scale hydrogen production *via* photoelectrochemical water splitting has been reported.[9] Due to their very similar compounds, an additional perk for dye-sensitised systems is that discoveries made in the area of dye-sensitised solar cells can readily be transferred to DS-PCE for hydrogen production and *vice versa*. Furthermore, in contrast to most other technologies, dye-sensitised light harvesting systems can work under diffuse and dim-light conditions, since they do not depend as much on the angle of light incidence.[10] The latter makes them – together with perovskite solar cells – also ideal for application of portable electronics and the Internet of Things (IOT).[11] Despite the rise of perovskite solar cells over the last few years and their impressive increase in performance, the attractiveness of dye-sensitised solar harvesting systems has not faded due to their transparency and wide colour variety, as well as their fabrication from earth abundant materials at relatively low temperatures.

2.2 Dye-sensitised solar harvesting devices

In comparison to the previously mentioned solar harvesting devices, the advantage of dye-sensitised systems lies in their versatility and tunability which is harder to achieve with other renewable energy devices. The spectral response and dye energy positions with regard to the chosen semiconductor can be easily adjusted by changing the dye structure, along with the colour of the device. Their variety of substrates as well as their ability to work under varying lighting conditions and shaded, diffuse light make them attractive for low density and indoor applications. In addition to their transparency, this gives dye-sensitised devices unique areas of application and they can be considered a green technology due to their aforementioned low energy manufacturing demand and fabrication from abundant resources.

Despite their promising future, dye-sensitised solar harvesting devices are lagging behind due to their relatively low efficiency

which has not increased as drastically over the last decade as it has for other technologies. Despite the fact that the most efficient dye-sensitised solar cell is currently an n-type dye-sensitised device based on a liquid electrolyte (14% reported record efficiency[12]), devices with a solid-state electrolyte have several advantages, such as the prevention of leakage, evaporation or dye desorption, and, maybe most importantly, a much cheaper device fabrication route for large-scale applications, printing, as well as opening the possibility of leakage free flexible devices.[13–15] Unfortunately, these advantages usually come with a lower overall performance due to a faster charge recombination.[16,17]

The basic working principle of dye-sensitised solar energy conversion devices is either (i) for n-type: the injection of an electron from the excited dye into the conduction band of the sensitised semiconductor and consecutive oxidation of the electrolyte (or catalyst/water for solar fuel devices) and (ii) for p-type: the injection of a hole from the excited dye into the valence band of the sensitised semiconductor, as illustrated in Fig. 5. For a solar cell, the oxidised or reduced dye regenerated by the redox mediator (electrolyte), which then is regenerated through the counter electrode. Through this process, the electrons and holes move in opposite directions, facilitating charge separation and generating a photocurrent. The magnitude of the photocurrent depends on the number of dye molecules that absorb light and the dye utilisation factor, or more generally, how much absorbed light is converted into a current. The open circuit voltage (V_{oc}) of a single cell is the potential difference between the redox mediator and the Fermi level of the semiconductor (Fig. 5). For a DS-PEC water splitting device, a catalyst is typically co-immobilised on the semiconductor surface that facilitates either oxygen evolution (for n-type) or hydrogen evolution (for p-type).

One way to immensely boost the theoretical efficiency of dye-sensitised solar harvesting devices is to combine the n-type dye sensitised device (based on a n-type semiconductor) with a p-type dye-sensitised device (based on a p-type semiconductor) into a tandem dye-sensitised solar harvesting device. This potential advancement in dye-sensitised solar harvesting devices is the reason why p-type dye-sensitised devices have gained increasingly more attention despite their poor performance. Both DS-PEC and DSSCs would greatly benefit from a tandem system; a tandem DS-PEC would be able to achieve full water splitting without a traditional counter electrode (usually Pt).

For dye-sensitised solar cells, the ultimate goal would be to develop tandem solid state DSC devices (t-ssDSC) by exchanging the liquid electrolyte with a solid state charge transport material. Such a tandem device would no longer share the same redox mediator and electrolyte, instead each photoelectrode would have its own charge-transport material to replace the electrolyte. By connecting the photoelectrodes with a transparent and conductive layer to perform inner charge transfer, such a tandem solid state dye-sensitised solar cell, as illustrated in Fig. 5, would be able to reach a much higher V_{oc} and no longer be limited by the potential difference of the two semiconductors, leading to a proposed efficiency of up to 18% with a potential of 2 V based on complementary light absorption of the dyes on both photoelectrodes.[18]

Due to the aforementioned potential of tandem devices, developing p-type dye-sensitised solar harvesting devices is crucial to emerge into a new era for dye-sensitised systems, boosting the efficiency considerably while still remaining a low-cost photoconversion device with all the previously discussed advantages. Currently, the fabrication of a tandem device with high efficiency is still hindered by the poor performance of -type devices since a balanced photoanode and photoelectrode (p-type and n-type half cell) is required for such a device. The smallest photocurrent in the system will determine the overall photocurrent of the cell if connected in series. This means that the device can only be as efficient as the weaker half cell, which is problematic since the reported p-type efficiencies are significantly lower than their n-type counterparts.[19,20] Due to this immense application potential of p-type dye-sensitised solar harvesting devices, increasing their efficiency is crucial for the advancement for dye-sensitised solar cells and solar fuel devices in general.

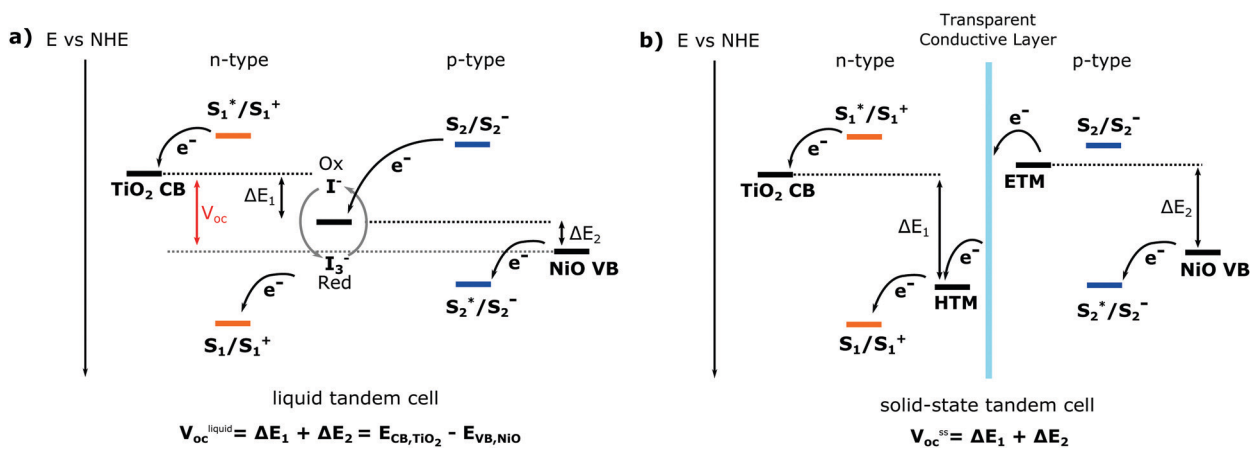

Fig. 5 Potential diagram of (a) the liquid based t-DSCs and (b) tandem solid state DSC where the liquid electrolyte is replaced by a solid-state hole transport material (HTM) for n-type cells and an electron transport material (ETM) for p-type cells.

While this perspective focuses on the semiconductor materials, it should be noted that there are multiple ways to improve the efficiency, and focusing on the individual components as well as their interaction is significant to move forward. Advances in the dyes,[21–26] electrolytes[19,21,27–29] or in general[17,21] can be found in the literature.

3 Semiconductor challenges for p-type dye-sensitised photocathodes

While the selection of earth abundant and 'green' elements with a low environmental impact is important for the large-scale feasibility, this does not guarantee that the final material or device will be cheap and green. The total impact of the cell is the sum of the various steps that need to be considered for the eco-efficiency of the final system: (i) the processing of raw materials for the chemical composition, (ii) the synthesis process for all components, (iii) the implementation into the system and (iv) the disassembly and recycling of all materials.[30]

3.1 Chemical composition

The ideal p-type semiconductor metal oxide for photocathodes used in dye-sensitised solar cells would be transparent to ensure maximal absorption of light by the dye, exhibit large hole mobility and stability, as well as a deep valence band position to increase the possible open circuit voltage (V_{oc}). For photoelectrochemical cells for solar fuel production, the semiconductor can be transparent and work similarly to a traditional dye-sensitised solar cell where all light is absorbed by the dye, and may also be a narrow band gap semiconductor that absorbs visible light. Upon illumination, the semiconductor can then transfer electrons into the co-catalyst on the surface with the dye acting as an additional light harvesting pathway. While not realised yet and unconventional in the traditional definition of dye-sensitised solar cells, narrow band gap semiconductors could also be utilised that inject electrons into the dye or electrolyte/solid-state electron transporting material, or in other words, a p/n-junction with the dye as the additional light harvester.

However, regardless of the final utilisation, good p-type metal oxide semiconductors are scarce due to fundamental reasons: for most p-type metal oxide semiconductors, the valence band is dominated by localised oxygen 2p orbitals, which leads to a high probability for the hole to be localised around the oxygen atoms and ultimately to poor hole mobility due to the need to overcome a large energy barrier to migrate.[31–33]

The search for efficient dye-sensitised photocathodes over the years has led to the exploration of other p-type semiconductor materials besides NiO, which is the most common semiconductor for p-type dye-sensitised photocathodes, both in solar cells and photoelectrochemical cells. Due to its large band gap of 3.6–4.0 eV,[38] NiO exhibits good transparency for thin films, despite the underlying brown colour due to Ni^{3+} ions that are present as a result of Ni^{2+} vacancies that form during sintering.[21] In an investigation of a range of different mesoporous NiO electrodes prepared by different research groups, Gibson *et al.*[39] could show that the performance of NiO depends on not only the crystallite size and film thickness but also on sintering temperature, all of which influence the crystallinity and surface states. Furthermore, Hammarström *et al.*[40] found out that these surface states are involved in hole trapping and act as tunnelling sites on a sub-ps timescale which lead to rapid recombination with the redox mediator. The issues mentioned above hint at the various challenges that are connected to make efficient photocathodes with this earth abundant material. Despite NiO being the most common p-type semiconductor for dye-sensitised photocathodes, NiO exhibits a high density of traps and a low hole mobility, and therefore small diffusion length for holes, leading to fast charge recombination.[41]

3.1.1 p-Type semiconductors beyond NiO. Alternative p-type semiconductor materials beyond NiO have been studied due to the previously mentioned challenges with NiO. While this is not aimed to be a complete list of p-type semiconductor materials that have been considered, we aim to provide an overview of a few promising NiO alternatives.

Among those studied are the earth abundant binary copper oxides, CuO and Cu_2O. The former has a comparably small optical band gap (see Fig. 6), thus making it less transparent, but has gathered attention due to its ease of fabrication, higher conductivity and good stability. In contrast, Cu_2O has a wider band gap but suffers from stability issues.[42] Cuprous and cupric oxides as well as their heterojunctions have been used repeatedly for photocatalytic H_2 production with a high conversion efficiency,[43,44] and n-type dye sensitised CuO/TiO_2 cells have been employed for hydrogen generation.[45] However no p-type dye-sensitised PEC devices have yet been reported to our knowledge. Nonetheless, Lu *et al.*[46] have managed to prepare Cu_2O films for p-type dye-sensitised solar cells with a reasonable voltage of 710 mV and a photon-conversion efficiency (PCE) of 0.42% with a liquid electrolyte. One of the most

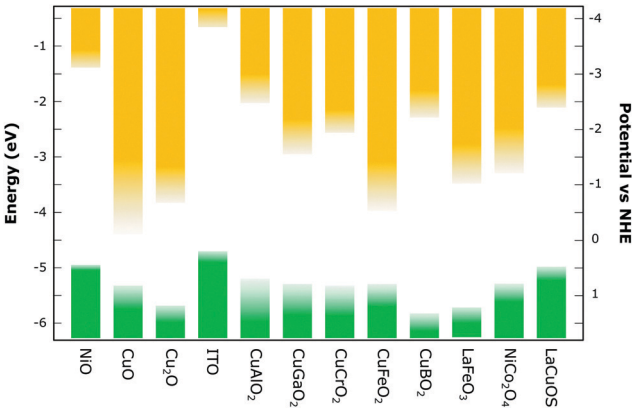

Fig. 6 Selection of reported parameters for various p-type metal-oxide semiconductors which have also been utilised in p-type dye-sensitised solar cells. Exact values can differ depending on synthesis methods and testing conditions used. This is indicated by the 'fading' of the band positions – a larger fade-out represents a larger difference of the reported band positions. A graph was made with data from the literature.[21,34–37]

transparent metal oxides is n-type degenerate tin-doped indium oxide (ITO) that has shown to be able to both accept and donate electrons from and to the photosensitiser if dye-coated.[47,48] Unfortunately, indium is one of the critical elements in the periodic table (Fig. 2), otherwise its low sheet resistance and relatively low temperature preparation (see Fig. 7) make this an attractive metal oxide. Huang *et al.*[47] have intensely studied ITO with p-type dyes for p-DSCs and Bach *et al.*[49] were able to fabricate a liquid p-DSC based on ITO films with a PCE of up to 2%, which is close to that of the best reported analogous NiO devices. Additionally, the group of Meyer *et al.* was able to fabricate a photocathode with ITO with a "donor–dye–catalyst" assembly for water reduction with an increased hydrogen evolution efficiency compared to simple dye–catalyst structures on p-type metal oxides.[50]

Another group of semiconductor materials that have attracted much attention recently are ternary oxides, especially copper oxides ($CuMO_2$ with M = B, Al, Ga, Cr, Fe...). Not only do these delafossite Cu(I) ternary oxides consist of earth abundant elements but also additionally benefit from favourable cation size and the mixing of the d-states of the M(III) ions with the oxygen p orbitals and reduce the hole localisation through orbital hybridisation in contrast to most other metal oxides that suffer from low hole mobility due to localised oxygen 2p orbitals.[51] The typical delafossite structure has two polytypes that depend on the stacking of alternating layers of MO_6 octahedra and two-dimensional packed Cu^+ ions. The polytype with rhombohedral symmetry is referred to as "3R" (space group *R*3*m*) and the "2H" polytype with an alternating stacking sequence (space group *P*63/*mmc*).

Due to its large band gap and thus high transparency, $CuAlO_2$ has been intensely studied for solar harvesting devices in the past decade. While $CuAlO_2$ has been shown to work for dye-sensitised solar cells, the PCE of the devices is comparably small.[57–59] The low performance is largely a result of the synthesis, where for example a large particle size leads to low dye loading and consequently low photocurrent. However, even with smaller $CuAlO_2$ nanoparticles, reaching higher efficiencies is still challenging. More recently, a study by Ursu *et al.*[60] that investigated the effect of polymorphism showed that the presence of the 2H-$CuAlO_2$ polytype in small concentration increased the efficiency compared to the pure 3R polytype. Photocatalytic hydrogen evolution has been achieved over $CuAlO_2$,[61,62] but has not yet been realised with the addition of a dye.

Other popular delafossite Cu(I) ternary oxides are $CuGaO_2$ and $CuCrO_2$ due to their large band gap. Comparably, the band gap of the iron (making this material very earth abundant) analogue $CuFeO_2$ is small, resulting in a strongly absorbing semiconductor which decreases the amount of light absorbed by the dye, consequently decreasing the photocurrent (see Fig. 6).[73,74] Zhu *et al.*[63] have reported a p-DSC with $CuFeO_2$ that was able to reach a significant photovoltage but only reached a photocurrent of 71 μA cm^{-2}. Despite not reaching record efficiencies, liquid p-DSCs fabricated with $CuGaO_2$,[66] as well as $CuCrO_2$[64,75] have been reported to reach comparable efficiency values to analogue DSCs based on NiO under similar conditions which shows the potential of these materials. Solar hydrogen production has been realised for non-dye sensitised $CuGaO_2$[76–78] and $CuCrO_2$[79,80] as well as Ru(II)–Re(I) supramolecular photocatalysts sensitised on the $CuGaO_2$ surface.[67] For $CuCrO_2$, Reisner *et al.*[65,81] have successfully prepared photocathodes for water splitting with coimmobilised p-type organic dyes and a phosphonated molecular Ni catalyst. Similar to the other delafossite Cu(I) oxides, the reported dye-photocathodes of $CuBO_2$ for solar cells showed a smaller photocurrent due to a low specific surface area but showed promise with a larger photovoltage than the NiO comparable device;[68] however photocathodes for water splitting have not been reported. It should be noted that investigations on charge-transfer processes with different driving forces (that arise with alternative metal oxides) could show that insufficient driving forces could hinder hole injection from the dye into the semiconductor.[21] This underlines the importance of tailoring the sensitisers to the individual semiconductor metal oxides and their properties, which could pave the way for more efficient photocathodes.

Unlike most of the aforementioned p-type metal oxide semiconductors, perovskite lanthanum iron oxide ($LaFeO_3$) has not been employed for solar cells but only in dye-sensitised photoelectrochemical cells for H_2 generation.[69] It has a suitable band gap in the range of 2.1 to 2.6 eV, and absorbs visible light and exhibits high stability under illumination in aqueous solutions, making it interesting for solar hydrogen production.[37,82] Sun *et al.*[69] utilised the molecular dye and phosphonated molecular Ni as the hydrogen production catalyst (NiP) and could show that the dye-sensitised photocathode (NiP + dye)@$LaFeO_3$ outperformed the non-sensitised NiP@$LaFeO_3$ photocathode due to light absorption by both the molecular dye and $LaFeO_3$.

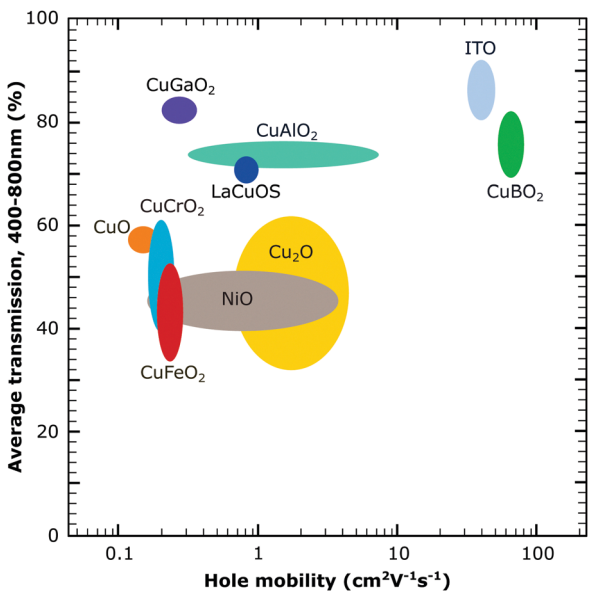

Fig. 7 Comparison of the several p-type metal oxides from the literature showing transmission over the visible range and hole mobility. The larger circles indicate a larger variation of the reported values for the materials. The figure was obtained with data from the literature.[21,52–56]

An additional type of p-type semiconductor is the group of oxysulfides, which replace oxygen with a chalcogen in order to overcome the hindrance of localised oxygen p-orbitals that decrease charge mobility.[83] One representative of this group is LaCuOS, which has a higher conductivity and transparency than NiO and can be successfully synthesised by a low temperature solvothermal method.[84] Jobic *et al.*[70] demonstrated the successful implementation of LaOCuS as a photocathode in p-DSSCs, however showed several synthetic challenges and low surface area as well as poor binding affinity for the dye, which is why ternary oxides might currently be considered a more promising approach.

Another material class worth mentioning are the spinel structures, AB_2O_4 (for example $NiCo_2O_4$) falls into this class of p-type semiconductors, which has a reported higher conductivity than NiO.[85] The fabrication of a p-DSC with $NiCo_2O_4$ nanowire–nanosheet arrays sensitised with a ruthenium dye yielded relevant photo-conversion efficiency (PCE = 0.78%), which shows the potential of spinel semiconductors.[71,86] While $NiCo_2O_4$ has been utilised for solar hydrogen production,[87,88] DS-PEC cells have not been investigated yet. The second spinel that has been tested for dye-sensitised systems is $CuFe_2O_4$, which was used by Li *et al.*[72] for photoelectrochemical cells and was able to reach a decent efficiency.

The summarised standard solar cell and solar fuel data for the current metal oxide semiconductor materials beyond NiO in Table 1 show that a lot of materials are still left unexplored for dye-sensitised systems as well as the low photocurrent for all p-type semiconductors. This can be related to the low hole conductivity in the discussed materials as shown in Fig. 7 as well as a low surface area for some of the reported materials. The photocurrent is especially meaningful for the successful development of tandem dye-sensitised solar harvesting devices and finding strategies to improve the photocurrent will be the main challenge in reaching this goal. For materials with a lower charge conductivity, the electrode design and structure will play an important role and are briefly discussed in the following sections.

Other materials worth mentioning due to their elemental abundance and have not been utilised for dye-sensitised devices but have been reported for water splitting are $CuNbO_3$[89,90] with a band gap of 2 eV that has been reported for hydrogen evolution and other spinel type p-type semiconductors such as $CuAl_2O_4$[91] and $CuMn_2O_4$ that have been less common for photocatalysis.[92]

In addition to p-type semiconductor materials currently under development, it should be noted that computational studies can aid in finding and developing novel conductive p-type metal oxides with desired properties. For example, K. Yim *et al.*[33] conducted a high-throughput screening for binary and ternary oxides to identify promising p-type transparent metal oxides.

Generally, while all of these materials have not yet exceeded NiO based photocathode efficiencies, it is important to keep in mind that NiO has been studied for a much longer time for dye sensitisation and its aspects (*e.g.* surface states and recombination pathways) are still not fully understood in dye-sensitised systems.

Table 1 Summarised standard solar cell and solar fuel data of current p-type metal oxide semiconductor materials beyond NiO in dye-sensitised photocathodes. Tabulated are the best performing photocathodes for each material. For DSCs, the utilised electrolyte, short-circuit current density and photoconversion efficiency are noted, whereas for DS-PEC, the catalyst, photocurrent and faradaic efficiency are noted. For the blank rows, to our knowledge, no data have been reported at present

		Dye	Electr./cat.	V_{oc} (mV)	J (mA cm^{-2})	η_{PCE}/η_F
Cu_2O	DSC	C343	I_3^-/I^-	710	1.30	0.42[46]
	PEC					
ITO	DSC	Ru-8T	$Fe^{2+/3+}$	712	5.65	1.96[49]
	PEC	RuP2-DA	NiP		0.06	53[50]
$CuAlO_2$	DSC	Ru-6T	I_3^-/I^-	333	0.30	0.04[58]
	PEC					
$CuFeO_2$	DSC	C343	I_3^-/I^-	365	0.07	0.01[63]
	PEC					
$CuCrO_2$	DSC	PMI-6T-NDI	$Co^{2+/3+}$	734	1.23	0.48[64]
	PEC	PMI-P	NiP		0.03	41[65]
$CuGaO_2$	DSC	PMI-NDI	$Co^{2+/3+}$	305	0.42	0.05[66]
	PEC	RuRe	RuRe		0.02	72[67]
$CuBO_2$	DSC	DPP-NDI	$Co^{2+/3+}$	453	0.02	0.001[68]
	PEC					
$LaFeO_3$	DSC					
	PEC	P1*	NiP		0.02	45[69]
LaOCuS	DSC	PMI-NDI	$Co^{2+/3+}$	150	0.04	0.002[70]
	PEC					
$NiCo_2O_4$	DSC	N719	I_3^-/I^-	189	8.35	0.79[71]
	PEC					
$CuFe_2O_4$	DSC					
	PEC	MnTPP	—		0.01	53[72]

Nonetheless, it can be concluded that alternative p-type semiconductor materials beyond NiO are promising but need further optimisation for dye-sensitised photocathode application, as well as further investigation of the underlying charge transport processes is needed.

3.1.2 Core–shell structures. With the recent increased attention of core–shell nanoparticles for a broad range of applications in catalysis and materials chemistry,[93] it is of little surprise that these structures have made it in the field of dye-sensitised photocathodes. Almost at the same time, two core–shell structures were reported for dye-photocathodes: Cu_2O@CuO by Jobic *et al.*[94] in 2018 and NiO–dye–TiO_2 with Al_2O_3 as the inner barrier by our group[95] in 2017.

As previously mentioned, Cu_2O is considered an attractive p-type semiconductor for dye-sensitised photocathodes both due to the deeper valence band and higher conductivity than NiO, but its instability limits the conversion efficiency of such devices and makes it unsuitable for water splitting. The idea behind the Cu_2O@CuO core–shell structure was to overcome the chemical instability of Cu_2O and utilise CuO as a passivating layer which has been proven to be successful.[94] This thin outer layer (5 nm thickness) was also shown to facilitate the transfer of holes from CuO to Cu_2O to increase the injection efficiency of the excited dye and indicates the potential of such core–shell systems for photocathodes.

For the NiO–dye–TiO_2 core–shell structure, our motivation was to design a ''well-oriented'' structure (see Fig. 8) to facilitate injection efficiencies.[95] The donor and acceptor of the designed dye should be close to their respective semiconductors, *i.e.* the electron donor part of the dye close to p-type NiO and the electron

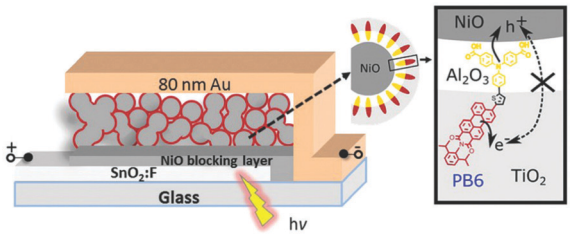

Fig. 8 The configuration and working principle of the p-type dye sensitised NiO–dye–TiO_2 core–shell solar cell, NiO–PB6–Al_2O_3–TiO_2, with Al_2O_3 as an inner barrier layer and donor–π–acceptor dye PB6 as a photosensitiser. Taken from ref. 96.

acceptor part close to n-type TiO_2 to get fast and efficient hole and electron injection from the dye upon light illumination. This architecture led to efficient and ultrafast hole injection (>98%, ≤200 fs) as well as unprecedentedly fast dye regeneration (70–93%, ≤500 fs) and the recombination in such a core–shell NiO–dye–TiO_2 structure was found to be much slower than that of the conventional dye sensitised NiO film. An additional Al_2O_3 inner barrier layer between NiO and TiO_2 was shown to suppress charge recombination and prolong charge lifetime in the dye-sensitised film.[96] Further studies by our group[97] suggested that the low photocurrent is mainly due to the low utilisation fraction of the dyes of <5%, meaning that most of the dyes do not contribute to photocurrent in this system. The reason for this is that the solid electrolyte, or rather TiO_2 in this case, is not electronically well connected and most of the injected electrons are trapped in unconnected electron conductors that do not contribute to the photocurrent. A unity dye utilisation factor for the same devices would improve the photoconversion efficiency significantly (up to 4%), which suggests that improving the dye utilisation is a key challenge for unlocking efficient solid-state p-type DSCs.

3.1.3 Morphology and electrode design. When comparing the different material choices for dye-sensitised photocathodes, it is important to keep in mind that the electrode morphology and topography play an important role in the performance of the cell. While the choice of material will mostly influence the photovoltage which is related to the energy levels of the used components, the photocurrent is greatly affected by the electrode structure, for example the porosity or nanostructure. A lot of the previously discussed semiconductor materials have not been extensively studied or tailored to the needs of dye-sensitised systems which is one of the reasons for the low reported photoconversion efficiency and a large particle size, low surface area or low dye loading limits their photocurrent. For n-type semiconductors, 0-D and 1-D (and even 2-D) nanostructures or the combination of the two have been shown to enhance the performance for dye-sensitised systems.[98] Nanotubes or nanowire arrays have the advantage of providing a direct path for charge transport with fewer grain boundaries and better charge mobility (up to several orders of magnitude) while also providing a large surface area.[98] Consequently, the exploration and rational design of electrode materials are key to improve the efficiency of solar energy conversion devices, as well as to investigate how charges diffuse through the electrode material. Both theoretical calculations as well as novel synthesis routes need to be employed to develop efficient photocathode materials.

3.2 Synthesis and film deposition

Since the energy demand of the synthesis process can greatly affect the eco-efficiency, as previously discussed for crystalline-Si solar cells, replacing high temperature synthesis methods with low temperature processes is crucial to further decrease the cumulative energy demand for the upcoming solar harvesting devices. Lowering the synthesis temperature of photocathode materials has several benefits, which are illustrated in Fig. 9. Not only do low temperature methods save energy, but shifting from high temperature synthesis routes, which are typical for

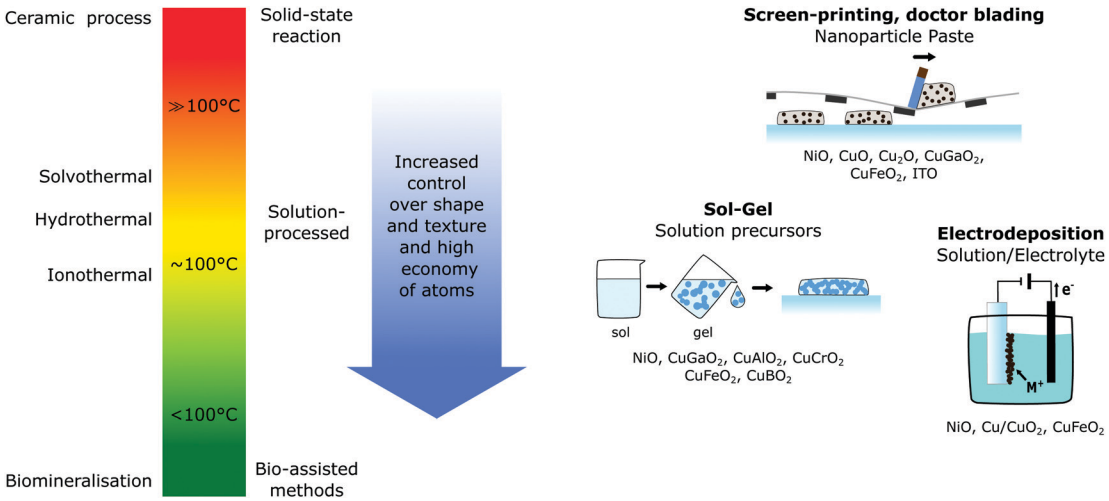

Fig. 9 As the synthesis temperature is decreased, there are several benefits beyond saving energy such as more control over shape and texture. Current film deposition methods that are most important for dye-sensitised devices are illustrated along with the semiconductor materials that have been reported for these methods.

solid-state reactions, towards solution based methods (hydro-, solvo- and ionothermal) or even lower temperature bio-assisted methods, increases the control of shape, size and purity of the materials.[30]

Currently, most p-type semiconductor materials require relatively high temperature synthesis routes, typically with temperatures between 300 and 900 °C[52,99] which underlines the need to develop new low-temperature synthesis methods for this type of material. Along with the temperature, the film deposition technique and growth or metal oxide thin films is the most significant factor that determines the structural, optical and electrical properties.[32] Slight variations in the parameters even for the same technique can result in different properties, as shown in the previously mentioned investigation of mesoporous NiO electrodes prepared by different research groups.[39]

While there is a broad variety of synthesis methods for p-type transparent semiconductors,[32,100] electrodes for dye-sensitised solar energy conversion require mesoporous semiconductor thin films with a high surface area (and a minimal number of grain boundaries for solar cells) to accommodate a maximal number of dye molecules (or active surface sites for (photo)catalysis) and thus, there are fewer reported deposition methods. Despite there still being a multitude of methods, the main methods for p-type dye-sensitised photocathode preparation can be narrowed down to screen printing,[39,63,101] solution processed routes (which include sol–gel,[39,101,102] inkjet printing[21,103] and spray pyrolysis[37]) or electrodepostion.[62,104] All of these methods are capable of large scale deposition of uniform thin films compatible with flexible substrates, such as conductive PET.[105]

One of the two most common deposition methods is based on a paste of premade nanoparticles (typical size 15–60 nm[39,101,106]) of the desired semiconductor in an ethyl-cellulose solution, which is transferred onto the substrate through doctor blading or screen-printing, where the paste is pushed through a mesh, before a necessary calcination step (typically 200–500 °C).[39,101] Here, the fabrication of the initial nanoparticles, the preparation of the paste and the calcination temperature greatly influence the semiconductor film properties, making it hard to control fully and reproducibility across batches can be hard. However, due to its ease of fabrication and large-scale applicability, screen-printing has been reported for various p-type mesoporous semiconductors for dye-sensitised applications for NiO,[39] CuO, Cu_2O,[107] $CuGaO_2$,[66] $CuFeO_2$,[63] $CuCrO_2$,[75] and ITO. Despite the ease of application and fabrication, this method requires two heating steps, for the nanoparticle synthesis and the calcination step, and is therefore not very energy efficient. The other common deposition method, sol–gel, which is part of the multitude of solution processed fabrication routes, only required one heating step, making this method more energy efficient. Typical precursors used are metal alkoxides in a colloidal solution (sol) that are transformed into a network (gel), most often with the help of polymers. Subsequent annealing at 300–500 °C yields a mesoporous film. This process is particularly common for most ternary oxides[68,74,102,108] as well as NiO.[39,109–111]

Whereas electrodeposition is very common for photoelectrodes for water splitting without a dye for a few of the previously mentioned semiconductors,[62,104,112] this method has not been applied to dye-sensitised photocathodes. Only for NiO[104,113] and Cu/Cu_2O,[114] dye-sensitised systems have been reported. While electrodeposition is generally easy to control in terms of film thickness, coverage and porosity can be a challenge for this method and post-treatment is typically required; however Sonavane *et al.*[115] have reported the electrodeposition of NiO films without necessary heat post-treatment.

With very few exceptions, all of the reported fabrication methods need an annealing or post-treatment heating step that is required to achieve crystalline semiconductor particles, and moving towards even lower synthesis routes shown in Fig. 9 due to the aforementioned advantages is desirable. For NiO synthesis, hydrothermal and solvothermal methods have been investigated that use water or alcohols, respectively, as solvent that is heated typically to 180–220 °C.[116] Knowles *et al.*[117] recently reported a novel synthesis route for phase-pure colloidal NiO nanocrystals through direct solvothermal synthesis. This also eliminated the need for commonly used postsynthetic modification steps, such as oxidation or calcination and illustrates the importance of investigating novel synthesis approaches to increase synthesis control and save energy.

4 Conclusions

Dye-sensitised solar harvesting devices are largely based on earth abundant materials, which make them a viable candidate for sustainable solar energy conversion. In order to overcome current limitations in device performance, p-type dye-sensitised solar harvesting devices are necessary to make tandem cells. However, achieving a transparent and hole conductive p-type semiconductor film for dye-sensitisation is currently one of the biggest challenges. Nonetheless, a multitude of earth abundant metal oxides have been investigated that show promise but also hurdles of p-type semiconductors that need to be overcome to reach the market stage.

In order to reach the goal of synthesising a p-type dye-sensitised system that can keep up with the n-type counterpart, the focus will be mainly on improving the photocurrent, which is greatly lagging behind. This can be reached through a rational electrode design as well as developing organic dyes that are tailored to the individual needs of the chosen p-type semiconductor. Potential breakthroughs are likely to come from the development of new dyes as well as semiconductor materials beyond NiO, which is currently the standard p-type semiconductor but has inherent drawbacks due to its trap states that are promoting charge recombination and insufficient charge mobility. The development of semiconductors as well as finding a suitable synthesis and fabrication method will most likely be a key component in reaching the goal of efficient photocathodes.

Today, concerns regarding the sustainability of solar harvesting devices are steadily increasing due to the necessary

large scale of devices that need to be employed over the next decade to address the ever increasing energy demand. While life-cycle assessment of systems already on the market is becoming more popular, newer technologies still in the research state are less investigated. However, even for emerging technologies, the sustainability and fabrication costs are considered equally important as the pure efficiency of the devices. While our society is becoming more aware of the importance of sustainability and undoubtedly large advances have been achieved, the question remains whether solar harvesting devices can emerge from the research stage to large scale and relatively low cost fabrication quick enough to transition fully into CO_2-free electricity and fuel production in the next two decades while meeting the increasing energy demand.

Conflicts of interest

There are no conflicts to declare.

Acknowledgements

The authors acknowledge Uppsala University and the Swedish Energy Agency (49278-1) for financial support.

Notes and references

1 N. S. Lewis, *MRS Bull.*, 2007, 808–820.
2 IEA, World Energy Outlook 2019, OECD, 2019.
3 P. Breeze, *Power Generation Technologies*, Elsevier, 2019.
4 M. Tao, *SpringerBriefs in Applied Sciences and Technology*, Springer Verlag, 2014, pp. 9–20.
5 C. S. Tao, J. Jiang and M. Tao, *Sol. Energy Mater. Sol. Cells*, 2011, **95**, 3176–3180.
6 T. E. Graedel, E. M. Harper, N. T. Nassar, P. Nuss, B. K. Reck and B. L. Turner, *Proc. Natl. Acad. Sci. U. S. A.*, 2015, **112**, 4257–4262.
7 M. L. Parisi, S. Maranghi and R. Basosi, *Renewable Sustainable Energy Rev.*, 2014, **39**, 124–138.
8 J. W. Lee, J. Park and H.-J. Jung, *Energy Build.*, 2014, **81**, 38–47.
9 R. Sathre, C. D. Scown, W. R. Morrow, J. C. Stevens, I. D. Sharp, J. W. Ager, K. Walczak, F. A. Houle and J. B. Greenblatt, *Energy Environ. Sci.*, 2014, **7**, 3264–3278.
10 S. S. Y. Juang, P. Y. Lin, Y. C. Lin, Y. S. Chen, P. S. Shen, Y. L. Guo, Y. C. Wu and P. Chen, *Front. Chem.*, 2019, **7**, 209, DOI: 10.3389/fchem.2019.00209.
11 S. Yun, Y. Qin, A. R. Uhl, N. Vlachopoulos, M. Yin, D. Li, X. Han and A. Hagfeldt, *Energy Environ. Sci.*, 2018, **11**, 476–526.
12 K. Kakiage, Y. Aoyama, T. Yano, K. Oya, J.-I. Fujisawa and M. Hanaya, *Chem. Commun.*, 2015, **51**, 15894–15897.
13 G. Li, L. Sheng, T. Li, J. Hu, P. Li and K. Wang, *Sol. Energy*, 2019, **177**, 80–98.
14 D. Wei, H. E. Unalan, D. Han, Q. Zhang, L. Niu, G. Amaratunga and T. Ryhanen, *Nanotechnology*, 2008, **19**, 424006.
15 Z. Xue, C. Jiang, L. Wang, W. Liu and B. Liu, *J. Phys. Chem. C*, 2014, **118**, 16352–16357.
16 J. Zhang, M. Freitag, A. Hagfeldt and G. Boschloo, *Springer*, Singapore, 2018, pp. 151–185.
17 G. Boschloo, *Front. Chem.*, 2019, **7**, 77.
18 H. Tian, *Sustainable Energy Fuels*, 2019, **3**, 888–898.
19 I. R. Perera, T. Daeneke, S. Makuta, Z. Yu, Y. Tachibana, A. Mishra, P. Bäuerle, C. A. Ohlin, U. Bach and L. Spiccia, *Angew. Chem., Int. Ed.*, 2015, **54**, 3758–3762.
20 A. Carella, F. Borbone and R. Centore, *Front. Chem.*, 2018, **6**, 481.
21 E. Benazzi, J. Mallows, G. H. Summers, F. A. Black and E. A. Gibson, *J. Mater. Chem. C*, 2019, **7**, 10409–10445.
22 T. T. T. Pham, S. K. Saha, D. Provost, Y. Farré, M. Raissi, Y. Pellegrin, E. Blart, S. Vedraine, B. Ratier, D. Aldakov, F. Odobel and J. Bouclé, *J. Mater. Chem. C*, 2017, **121**, 129–139.
23 M. Bonomo, S. Sheehan, D. P. Dowling, L. Gontrani and D. Dini, *ChemistrySelect*, 2018, **3**, 6729–6736.
24 K. A. Click, D. R. Beauchamp, B. R. Garrett, Z. Huang, C. M. Hadad and Y. Wu, *Phys. Chem. Chem. Phys.*, 2014, **16**, 26103–26111.
25 F. Wu, J. Liu, X. Li, Q. Song, M. Wang, C. Zhong and L. Zhu, *Eur. J. Org. Chem.*, 2015, 6850–6857.
26 B. Xu, S. Wrede, A. Curtze, L. Tian, P. B. Pati, L. Kloo, Y. Wu and H. Tian, *ChemSusChem*, 2019, **12**, 3243–3248.
27 V. Nikolaou, A. Charisiadis, G. Charalambidis, A. G. Coutsolelos and F. Odobel, *J. Mater. Chem. A*, 2017, **5**, 21077–21113.
28 E. A. Gibson, A. L. Smeigh, L. Le Pleux, L. Hammarström, F. Odobel, G. Boschloo and A. Hagfeldt, *J. Phys. Chem. C*, 2011, **115**, 9772–9779.
29 H. Iftikhar, G. G. Sonai, S. G. Hashmi, A. F. Nogueira and P. D. Lund, *Materials*, 2019, **12**, 1998.
30 D. Larcher and J. M. Tarascon, *Nat. Chem.*, 2015, **7**, 19–29.
31 H. Kawazoe, H. Yanagi, K. Ueda and H. Hosono, *MRS Bull.*, 2000, **25**, 28–36.
32 A. Banerjee and K. Chattopadhyay, *Progress in Crystal Growth and Characterization of Materials*, 2005, vol. 50, pp. 52–105.
33 K. Yim, Y. Youn, M. Lee, D. Yoo, J. Lee, S. H. Cho and S. Han, *npj Comput. Mater.*, 2018, **4**, 17, DOI: 10.1038/s41524-018-0073-z.
34 K. Rajeshwar, M. K. Hossain, R. T. Macaluso, C. Janáky, A. Varga and P. J. Kulesza, *J. Electrochem. Soc.*, 2018, **165**, H3192–H3206.
35 E. Schiavo, C. Latouche, V. Barone, O. Crescenzi, A. B. Muñoz-García and M. Pavone, *Phys. Chem. Chem. Phys.*, 2018, **20**, 14082–14089.
36 B. A. Williamson, J. Buckeridge, N. P. Chadwick, S. Sathasivam, C. J. Carmalt, I. P. Parkin and D. O. Scanlon, *Chem. Mater.*, 2019, **31**, 2577–2589.
37 G. S. Pawar and A. A. Tahir, *Sci. Rep.*, 2018, **8**, 1–9.
38 E. L. Miller, *J. Electrochem. Soc.*, 1997, **144**, 1995.

39 C. J. Wood, G. H. Summers, C. A. Clark, N. Kaeffer, M. Braeutigam, L. R. Carbone, L. D'Amario, K. Fan, Y. Farré, S. Narbey, F. Oswald, L. A. Stevens, C. D. J. Parmenter, M. W. Fay, A. La Torre, C. E. Snape, B. Dietzek, D. Dini, L. Hammarström, Y. Pellegrin, F. Odobel, L. Sun, V. Artero and E. A. Gibson, *Phys. Chem. Chem. Phys.*, 2016, **18**, 10727–10738.

40 L. D'Amario, R. Jiang, U. B. Cappel, E. A. Gibson, G. Boschloo, H. Rensmo, L. Sun, L. Hammarström and H. Tian, *ACS Appl. Mater. Interfaces*, 2017, **9**, 33470–33477.

41 S. Mori, S. Fukuda, S. Sumikura, Y. Takeda, Y. Tamaki, E. Suzuki and T. Abe, *J. Phys. Chem. C*, 2008, **112**, 16134–16139.

42 O. Langmar, C. R. Ganivet, A. Lennert, R. D. Costa, G. De La Torre, T. Torres and D. M. Guldi, *Angew. Chem., Int. Ed.*, 2015, **54**, 7688–7692.

43 Z. Zhang and P. Wang, *J. Mater. Chem.*, 2012, **22**, 2456–2464.

44 D. Barreca, P. Fornasiero, A. Gasparotto, V. Gombac, C. Maccato, T. Montini and E. Tondello, *ChemSusChem*, 2009, **2**, 230–233.

45 Z. Jin, X. Zhang, Y. Li, S. Li and G. Lu, *Catal. Commun.*, 2007, **8**, 1267–1273.

46 S. Du, P. Cheng, P. Sun, B. Wang, Y. Cai, F. Liu, J. Zheng and G. Lu, *Chem. Res. Chin. Univ.*, 2014, **30**, 661–665.

47 Z. Huang, M. He, M. Yu, K. Click, D. Beauchamp and Y. Wu, *Angew. Chem., Int. Ed.*, 2015, **54**, 6857–6861.

48 Y. Furmansky, H. Sasson, P. Liddell, D. Gust, N. Ashkenasy and I. Visoly-Fisher, *J. Mater. Chem.*, 2012, **22**, 20334.

49 Z. Yu, I. R. Perera, T. Daeneke, S. Makuta, Y. Tachibana, J. J. Jasieniak, A. Mishra, P. Bäuerle, L. Spiccia and U. Bach, *NPG Asia Mater.*, 2016, **8**, e305.

50 B. Shan, A. K. Das, S. Marquard, B. H. Farnum, D. Wang, R. M. Bullock and T. J. Meyer, *Energy Environ. Sci.*, 2016, **9**, 3693–3697.

51 D. O. Scanlon, K. G. Godinho, B. J. Morgan and G. W. Watson, *J. Chem. Phys.*, 2010, **132**, 024707.

52 K. Fleischer, E. Norton, D. Mullarkey, D. Caffrey and I. V. Shvets, *Materials*, 2017, **10**, 1019.

53 S. Zhang, H. Ye, J. Hua and H. Tian, *Energy Chem.*, 2019, **1**, 100015.

54 M. I. Díez-García and R. Gómez, *ChemSusChem*, 2017, **10**, 2457–2463.

55 A. Liu, G. Liu, H. Zhu, B. Shin, E. Fortunato, R. Martins and F. Shan, *Appl. Phys. Lett.*, 2016, **108**, 233506.

56 L. Dong, G. Zhu, H. Xu, X. Jiang, X. Zhang, Y. Zhao, D. Yan, L. Yuan and A. Yu, *Materials*, 2019, **16**, 958.

57 J. Bandara and J. P. Yasomanee, *Semicond. Sci. Technol.*, 2007, **22**, 20–24.

58 A. Nattestad, X. Zhang, U. Bach and Y. Cheng, *J. Photonics Energy*, 2011, **1**, 011103.

59 J. Ahmed, C. K. Blakely, J. Prakash, S. R. Bruno, M. Yu, Y. Wu and V. V. Poltavets, *J. Alloys Compd.*, 2014, **591**, 275–279.

60 M. Miclau, N. Miclau, R. Banica and D. Ursu, *Mater. Today*, 2017, **4**, 6975–6981.

61 N. Koriche, A. Bouguelia, A. Aider and M. Trari, *Int. J. Hydrogen Energy*, 2005, **30**, 693–699.

62 S. Y. Choi, C. D. Kim, D. S. Han and H. Park, *J. Mater. Chem. A*, 2017, **5**, 10165–10172.

63 T. Zhu, Z. Deng, X. Fang, Z. Huo, S. Wang, W. Dong, J. Shao, R. Tao, C. Song and L. Wang, *J. Alloys Compd.*, 2016, **685**, 836–840.

64 S. Powar, D. Xiong, T. Daeneke, M. T. Ma, A. Gupta, G. Lee, S. Makuta, Y. Tachibana, W. Chen, L. Spiccia, Y.-B. Cheng, G. Götz, P. Bäuerle and U. Bach, *J. Mater. Chem. C*, 2014, **118**, 16375–16379.

65 C. E. Creissen, J. Warnan, D. Antón-García, Y. Farré, F. Odobel and E. Reisner, *ACS Catal.*, 2019, **9**, 9530–9538.

66 A. Renaud, L. Cario, P. Deniard, E. Gautron, X. Rocquefelte, Y. Pellegrin, E. Blart, F. Odobel and S. Jobic, *J. Mater. Chem. C*, 2014, **118**, 54–59.

67 H. Kumagai, G. Sahara, K. Maeda, M. Higashi, R. Abe and O. Ishitani, *Chem. Sci.*, 2017, **8**, 4242–4249.

68 T. Jiang, M. Bujoli-Doeuff, Y. Farré, E. Blart, Y. Pellegrin, E. Gautron, M. Boujtita, L. Cario, F. Odobel and S. Jobic, *RSC Adv.*, 2016, **6**, 1549–1553.

69 F. Li, R. Xu, C. Nie, X. Wu, P. Zhang, L. Duan and L. Sun, *Chem. Commun.*, 2019, **55**, 12940–12943.

70 A. Renaud, L. Cario, Y. Pellegrin, E. Blart, M. Boujtita, F. Odobel and S. Jobic, *RSC Adv.*, 2015, **5**, 60148–60151.

71 Z. Shi, H. Lu, Q. Liu, K. Deng, L. Xu, R. Zou, J. Hu, Y. Bando, D. Golberg and L. Li, *Energy Technol.*, 2014, **2**, 517–521.

72 X. Li, A. Liu, D. Chu, C. Zhang, Y. Du, J. Huang and P. Yang, *Catalysts*, 2018, **8**, 108.

73 C. G. Read, Y. Park and K. S. Choi, *J. Phys. Chem. Lett.*, 2012, **3**, 1872–1876.

74 M. S. Prévot, N. Guijarro and K. Sivula, *ChemSusChem*, 2015, **8**, 1359–1367.

75 D. Xiong, Z. Xu, X. Zeng, W. Zhang, W. Chen, X. Xu, M. Wang and Y. B. Cheng, *J. Mater. Chem.*, 2012, **22**, 24760–24768.

76 M. Lee, D. Kim, Y. T. Yoon and Y. I. Kim, *Bull. Korean Chem. Soc.*, 2014, **35**, 3261–3266.

77 T. Zhang, K. Zhu, M. Chen, T. Li, P. Li, Y. Cheng, Z. Zou, W. Luo and W. Huang, *J. Phys. D: Appl. Phys.*, 2019, **52**, 405501.

78 C. D. Windle, H. Kumagai, M. Higashi, R. Brisse, S. Bold, B. Jousselme, M. Chavarot-Kerlidou, K. Maeda, R. Abe, O. Ishitani and V. Artero, *J. Am. Chem. Soc.*, 2019, **141**, 9593–9602.

79 A. Varga, G. F. Samu and C. Janáky, *Electrochim. Acta*, 2018, **272**, 22–32.

80 S. Saadi, A. Bouguelia and M. Trari, *Sol. Energy*, 2006, **80**, 272–280.

81 C. E. Creissen, J. Warnan and E. Reisner, *Chem. Sci.*, 2018, **9**, 1439–1447.

82 I. M. Nassar, S. Wu, L. Li and X. Li, *ChemistrySelect*, 2018, **3**, 968–972.

83 H. Hiramatsu, K. Ueda, H. Ohta, M. Hirano, T. Kamiya and H. Hosono, *Appl. Phys. Lett.*, 2003, **82**, 1048–1050.

84 C. Doussier-Brochard, B. Chavillon, L. Cario and S. Jobic, *Inorg. Chem.*, 2010, **49**, 3074–3076.

85 I. T. Papadas, A. Ioakeimidis, G. S. Armatas and S. A. Choulis, *Adv. Sci.*, 2018, **5**, 1701029.
86 Z. Shi, H. Lu, Q. Liu, F. Cao, J. Guo, K. Deng and L. Li, *Nanoscale Res. Lett.*, 2014, **9**, 608.
87 L. An, L. Huang, P. Zhou, J. Yin, H. Liu and P. Xi, *Adv. Funct. Mater.*, 2015, **25**, 6814–6822.
88 J. Yin, P. Zhou, L. An, L. Huang, C. Shao, J. Wang, H. Liu and P. Xi, *Nanoscale*, 2016, **8**, 1390–1400.
89 U. A. Joshi, A. M. Palasyuk and P. A. Maggard, *J. Mater. Chem. C*, 2011, **115**, 13534–13539.
90 C. T. Crespo, *Sol. Energy Mater. Sol. Cells*, 2018, **179**, 305–311.
91 G. Li, C. Gu, W. Zhu, X. Wang, X. Yuan, Z. Cui, H. Wang and Z. Gao, *J. Cleaner Prod.*, 2018, **183**, 415–423.
92 S. Saadi, A. Bouguelia and M. Trari, *Renewable Energy*, 2006, **31**, 2245–2256.
93 M. B. Gawande, A. Goswami, T. Asefa, H. Guo, A. V. Biradar, D. L. Peng, R. Zboril and R. S. Varma, *Chem. Soc. Rev.*, 2015, **44**, 7540–7590.
94 T. Jiang, M. Bujoli-Doeuff, E. Gautron, Y. Farré, L. Cario, Y. Pellegrin, M. Boujtita, F. Odobel and S. Jobic, *J. Alloys Compd.*, 2018, **769**, 605–610.
95 L. Tian, J. Föhlinger, P. B. Pati, Z. Zhang, J. Lin, W. Yang, M. Johansson, T. Kubart, J. Sun, G. Boschloo, L. Hammarström and H. Tian, *Phys. Chem. Chem. Phys.*, 2017, **20**, 36–40.
96 L. Tian, J. Föhlinger, Z. Zhang, P. B. Pati, J. Lin, T. Kubart, Y. Hua, J. Sun, L. Kloo, G. Boschloo, L. Hammarström and H. Tian, *Chem. Commun.*, 2018, **54**, 3739–3742.
97 L. Tian, T. Törndahl, J. Lin, P. B. Pati, Z. Zhang, T. Kubart, Y. Hao, J. Sun, G. Boschloo and H. Tian, *J. Mater. Chem. C*, 2019, **123**, 26151–26160.
98 K. Yu and J. Chen, *Nanoscale Res. Lett.*, 2009, **4**, 1–10.
99 Y. J. Jang and J. S. Lee, *ChemSusChem*, 2019, **12**, 1835–1845.
100 A. Stadler, *Materials*, 2012, **5**, 661–683.
101 D. Dini, Y. Halpin, J. G. Vos and E. A. Gibson, *Coord. Chem. Rev.*, 2015, **304-305**, 179–201.
102 B. Satish and R. Srinivasan, *Mater. Today*, 2018, 2401–2411.
103 R. Brisse, R. Faddoul, T. Bourgeteau, D. Tondelier, J. Leroy, S. Campidelli, T. Berthelot, B. Geffroy and B. Jousselme, *ACS Appl. Mater. Interfaces*, 2017, **9**, 2369–2377.
104 S. Koussi-Daoud and T. Pauporté, *Oxide-based Materials and Devices VI*, 2015, p. 936425.
105 C. Glynn and C. O'Dwyer, *Adv. Mater. Interfaces*, 2017, **4**, 1600610.
106 M. Bonomo, N. Barbero, F. Matteocci, A. D. Carlo, C. Barolo and D. Dini, *J. Phys. Chem. C*, 2016, **120**, 16340–16353.
107 D. Ursu, M. Vajda and M. Miclau, *J. Alloys Compd.*, 2019, **802**, 86–92.
108 A. Alias, M. Sakamoto, T. Kimura and K. Uesugi, *Phys. Status Solidi C*, 2012, **9**, 198–201.
109 S. Sumikura, S. Mori, S. Shimizu, H. Usami and E. Suzuki, *J. Photochem. Photobiol., A*, 2008, **199**, 1–7.
110 N. N. M. Zorkipli, N. H. M. Kaus and A. A. Mohamad, *Procedia Chem.*, 2016, **19**, 626–631.
111 M. Jlassi, I. Sta, M. Hajji and H. Ezzaouia, *Surf. Interfaces*, 2017, **6**, 218–222.
112 C. G. Read, Y. Park and K. S. Choi, *J. Phys. Chem. Lett.*, 2012, **3**, 1872–1876.
113 S. Koussi-Daoud, A. Planchat, A. Renaud, Y. Pellegrin, F. Odobel and T. Pauporté, *ChemElectroChem*, 2017, **4**, 2618–2625.
114 F. Shao, J. Sun, L. Gao, J. Luo, Y. Liu and S. Yang, *Adv. Funct. Mater.*, 2012, **22**, 3907–3913.
115 A. C. Sonavane, A. I. Inamdar, P. S. Shinde, H. P. Deshmukh, R. S. Patil and P. S. Patil, *J. Alloys Compd.*, 2010, **489**, 667–673.
116 L. Qiao and M. T. Swihart, *Adv. Colloid Interface Sci.*, 2017, **244**, 199–266.
117 D. A. Brewster, Y. Bian and K. E. Knowles, *Chem. Mater.*, 2020, 1.